Neuronal apoptosis linked to EglN3 prolyl hydroxylase and familial pheochromocytoma genes: Developmental culling and cancer

Sungwoo Lee,[1,7] Eijiro Nakamura,[1,7] Haifeng Yang,[1] Wenyi Wei,[1] Michelle S. Linggi,[2] Mini P. Sajan,[3] Robert V. Farese,[3] Robert S. Freeman,[4] Bruce D. Carter,[2,5] William G. Kaelin, Jr.,[1,6,*] and Susanne Schlisio[1,7]

[1]Department of Medical Oncology, Dana-Farber Cancer Institute and Brigham and Women's Hospital, Harvard Medical School, Boston, Massachusetts 02115
[2]Department of Biochemistry, Vanderbilt University Medical School, Nashville, Tennessee 37232
[3]Department of Internal Medicine, James A. Haley Veterans Hospital and the University of South Florida College of Medicine, Tampa, Florida 33612
[4]Department of Pharmacology and Physiology, University of Rochester, Rochester, New York 14642
[5]Center for Molecular Neuroscience, Vanderbilt University Medical School, Nashville, Tennessee 37232
[6]Howard Hughes Medical Institute, Chevy Chase, Maryland 20815
[7]These authors contributed equally to this work.
*Correspondence: william_kaelin@dfci.harvard.edu

Summary

Germline *NF1*, *c-RET*, *SDH*, and *VHL* mutations cause familial pheochromocytoma. Pheochromocytomas derive from sympathetic neuronal precursor cells. Many of these cells undergo c-Jun-dependent apoptosis during normal development as NGF becomes limiting. *NF1* encodes a GAP for the NGF receptor TrkA, and *NF1* mutations promote survival after NGF withdrawal. We found that pheochromocytoma-associated *c-RET* and *VHL* mutations lead to increased JunB, which blunts neuronal apoptosis after NGF withdrawal. We also found that the prolyl hydroxylase EglN3 acts downstream of c-Jun and is specifically required among the three EglN family members for apoptosis in this setting. Moreover, EglN3 proapoptotic activity requires SDH activity because EglN3 is feedback inhibited by succinate. These studies suggest that failure of developmental apoptosis plays a role in pheochromocytoma pathogenesis.

Introduction

Pheochromocytomas are adrenal medullary tumors that are comprised of chromaffin cells, which are derived from sympathetic neuronal progenitor cells. Germline mutations in either *NF1*, *c-RET*, succinate dehydrogenase subunit genes (*SDHB*, *SDHC*, *SDHD*), or von Hippel-Lindau (*VHL*) are the most frequent cause of familial pheochromocytoma and are also common in seemingly sporadic pheochromocytoma (Maher and Eng, 2002; Neumann et al., 2002). In contrast, somatic mutations of these genes are rare in nonhereditary pheochromocytomas (Maher and Eng, 2002), raising the possibility that their functions must be altered during early development for pheochromocytomas to ensue.

Inheriting a defective *VHL* allele causes VHL disease, which is associated with an increased risk of hemangioblastomas, clear cell renal carcinomas, in addition to pheochromocytomas (Kaelin, 2002; Maher and Kaelin, 1997). Tumor development in this setting requires somatic loss of the remaining wild-type *VHL* allele in a susceptible cell. The *VHL* gene product, pVHL, is the substrate recognition unit of an E3 ubiquitin ligase complex that targets the α subunits of the heterodimeric transcription factor HIF (hypoxia-inducible factor) for proteasomal degradation (Kaelin, 2002; Schofield and Ratcliffe, 2004), and HIF appears to play a causal role in hemangioblastoma and clear cell renal carcinoma (Kim and Kaelin, 2004; Kondo et al., 2003; Zimmer et al., 2004). A number of other functions have been attributed to pVHL, but their relevance to pVHL-defective tumor formation is unclear (Czyzyk-Krzeska and Meller, 2004; Kaelin, 2002).

Several lines of evidence suggest that the role of pVHL in pheochromocytoma is qualitatively different from its role in

SIGNIFICANCE

Pheochromocytomas originate from neural crest cells that also form the sympathetic nervous system. Most of these cells normally die during development as growth factors such as NGF become limiting. Familial pheochromocytoma is genetically heterogeneous because it can be caused by *NF1*, *c-RET*, *SDH*, or *VHL* germline mutations. Mutations in these genes are rare in sporadic pheochromocytomas, however, unlike the usual Knudson two-hit scenario. Our findings explain these observations by linking the products of these genes to the induction of apoptosis following NGF withdrawal in assays thought to mirror developmental culling of neuronal progenitor cells. We also show that EglN3 prolyl hydroxylase activity is necessary for neuronal apoptosis in this setting and mechanistically link this activity to the mitochondrial enzyme SDH.

hemangioblastoma and renal carcinoma. First, biallelic *VHL* inactivation is common in sporadic hemangioblastoma and renal carcinomas but rare in sporadic pheochromocytomas (absent an occult germline *VHL* mutation), in violation of the Knudson two-hit model, wherein mutation of the same tumor suppressor gene is responsible for a hereditary cancer and its sporadic counterpart (the first mutation or "hit" of the two having occurred in the germline in hereditary cases) (Kim and Kaelin, 2004). This suggests that pheochromocytoma development in VHL disease is due to a $VHL^{+/-}$ field defect or reflects the loss of a critical pVHL function during development. Second, VHL disease can be subclassified based on the risk of pheochromocytoma (Zbar et al., 1996). Almost all *VHL* mutations linked to a high risk of pheochromocytoma (type 2 disease) are missense mutations, whereas null *VHL* mutations produce a low risk of pheochromocytoma (type 1 disease) (Zbar et al., 1996). This suggests that a mutant pVHL gain of function causes pheochromocytoma or that complete (rather than partial) loss of pVHL function is incompatible with pheochromocytoma development. Finally, some VHL families display a high risk of pheochromocytoma and a low risk of hemangioblastoma and renal cell carcinoma (type 2C disease). Type 2C pVHL mutants such as pVHL L188V appear to be normal with respect to HIF regulation (Clifford et al., 2001; Hoffman et al., 2001), suggesting that a pVHL target other than HIF is responsible for VHL-associated pheochromocytomas.

Hydroxylation of specific prolyl residues within the HIF-α subunits by EglN (also called PHD or HPH) triggers their recognition by pVHL (Kaelin, 2002; Schofield and Ratcliffe, 2004). EglN1 is the primary HIF-α hydroxylase under normal conditions in the many cell types examined to date, although all three EglN family members (EglN1, EglN2, and EglN3) can hydroxylate HIF-α in vitro (Berra et al., 2003; A. Bommi-Reddy and W.G. Kaelin, unpublished data; Bruick and McKnight, 2001; Epstein et al., 2001; Ivan et al., 2002). HIF dysregulation could, in theory, be the unifying feature of *VHL* and *SDH* mutations, since SDH inactivation would predictably attenuate prolyl hydroxylation in cells for the reasons outlined below (see Results). As described above, however, some pheochromocytoma-associated pVHL mutants appear to be normal with respect to HIF regulation (Clifford et al., 2001; Hoffman et al., 2001), implying that HIF-independent pVHL functions are linked to these tumors.

During embryogenesis, most sympathetic neuronal precursor cells undergo c-Jun-dependent apoptosis as growth factors such as nerve growth factor (NGF) become limiting (Estus et al., 1994; Ham et al., 1995; Schlingensiepen et al., 1994; Xia et al., 1995). Disease-associated *NF1* and *c-RET* mutations are known or suspected to enhance signaling by NGF receptors and promote neuronal survival (Dechant, 2002; Vogel et al., 1995). Here, we report that pVHL mutants linked to pheochromocytoma, including type 2C mutants, fail to downregulate the c-Jun antagonist JunB, which also promotes survival after NGF withdrawal. Moreover, the EglN1 paralog EglN3 (also called PHD3, HPH1, SM-20) is induced in sympathetic neurons after NGF withdrawal and provokes apoptosis when overexpressed in pheochromocytoma cells (Lipscomb et al., 1999, 2001; Straub et al., 2003). Based on these observations, we asked whether EglN3 might link SDH to neuronal survival under NGF limiting conditions. We found that EglN3, but not EglN1, is sufficient to induce neuronal apoptosis and does so in a hydroxylase-dependent manner. EglN3 acts downstream of c-Jun and is necessary for apoptosis after NGF withdrawal. SDH inactivation blocks neuronal apoptosis induced by EglN3 overproduction or NGF withdrawal. Therefore, all of the known familial pheochromocytoma genes affect a common pathway that culls sympathetic neuronal precursors during development.

Results

pVHL downregulates JunB

We recently discovered that mRNA levels for the secreted protein clusterin are attenuated in $VHL^{-/-}$ renal carcinoma cells (E. Nakamura et al., submitted). Notably, clusterin does not behave like a HIF target, and type 2C pVHL mutants, in contrast to wild-type pVHL, do not restore clusterin expression when reintroduced into such cells (E. Nakamura et al., submitted). The clusterin promoter contains binding sites for Myb, AP-1, and Sp1 (Cervellera et al., 2000; Herault et al., 1992; Jin and Howe, 1997). In pilot experiments, we found that wild-type, but not mutant, pVHL activated luciferase reporter plasmids containing the clusterin promoter unless the AP-1 site was destroyed (data not shown). This led us to examine the status of specific AP-1 family members in cells that do or do not contain wild-type pVHL. In electrophoretic mobility shift assays (EMSA), we detected increased AP-1 activity (Figure 1A; Figure S1 in the Supplemental Data available with this article online), due at least partly to JunB (Figure 1B), in renal carcinoma cells lacking wild-type pVHL. This effect was specific to JunB because the AP-1 family members c-Jun and c-Fos were not affected by pVHL in these assays (data not shown). JunB protein levels were also elevated in HeLa cervical carcinoma cells after elimination of pVHL with three independent siRNAs (Figure 1C and data not shown).

Regulation of JunB by pVHL involves both atypical protein kinase C and HIF

786-O $VHL^{-/-}$ cells produce HIF-2α but not HIF-1α (Maxwell et al., 1999). Type 2C pVHL mutants normalized HIF-2α levels when reintroduced into 786-O cells (Clifford et al., 2001; Hoffman et al., 2001) (see also Figures 2C and 7E) but did not normalize JunB levels (Figures 1D and 1E). Similarly, downregulation of HIF-2α in 786-O cells with short hairpin RNAs (shRNA) had little or no effect on JunB levels, in contrast to canonical HIF targets such as GLUT1 (Figure 2A). On the other hand, JunB was induced in cells containing wild-type pVHL that were engineered to produce a stabilized form of HIF-2α or treated with the hypoxia mimetic deferoxamine (DFO) (Figure 2B). Collectively, these results suggested that either JunB is already maximally stimulated at the residual HIF levels achieved with type 2C mutants or HIF-2α shRNA, or that regulation of JunB by pVHL involves HIF-dependent and HIF-independent pathways. The former possibility seems unlikely because JunB was not induced by DFO in cells producing the type 2C pVHL mutant L188V but was induced in cells producing wild-type pVHL, even though these cells produced nearly identical levels of HIF-2α and GLUT1 (Figure 2C).

The increased JunB protein levels observed in pVHL-defective cells, including those producing type 2C mutants, was associated with an ~2– to 3-fold increase in JunB mRNA levels (Figure S2). Transcription of JunB is regulated by atypical protein kinase C (PKC) family members (aPKC) (Kieser et al., 1996), and pVHL has been reported to polyubiquitinate aPKC

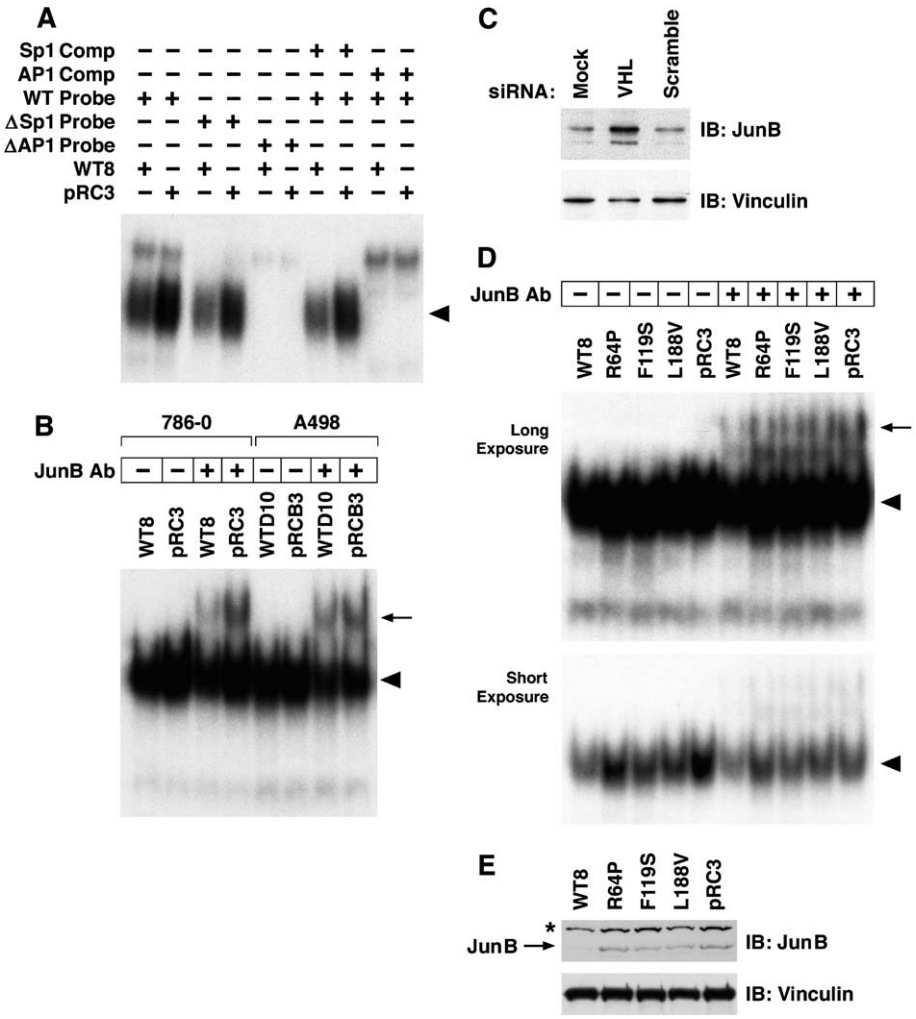

Figure 1. Increased JunB activity in pVHL-defective cells

A: Electrophoretic mobility shift assay (EMSA) with ^{32}P-labeled DNA probes spanning Sp1 and AP-1 sites in clusterin promoter and nuclear extracts prepared from 786-O *VHL*$^{-/-}$ renal carcinoma cells transfected to produce wild-type pVHL (WT8) or with empty vector (pRC3). WT, wild-type probe; ΔSp1, Sp1 site-mutated probe; ΔAP-1, AP-1 site-mutated probe. Where indicated, unlabeled DNA containing a canonical Sp1 or AP-1 binding site was added as a competitor (COMP). Arrowhead, AP-1 complex. **B and D:** EMSA with ^{32}P-labeled AP-1 site probe and nuclear extracts prepared from indicated cell lines. Anti-JunB antibody was added where indicated. Arrow, supershift complex. WTD10 and pRCB3 are A498 *VHL*$^{-/-}$ renal carcinoma cells transfected to produce wild-type pVHL or with empty vector, respectively. **D** includes 786-O cells transfected to produce pVHL R64P, L119S, or L188V. **C:** Immunoblot analysis of HeLa *VHL*$^{+/+}$ cervical carcinoma cells transfected with siRNA against VHL or scrambled siRNA. **E:** Immunoblot analysis of nuclear extracts used in **D**. Asterisk indicates nonspecific band.

(Okuda et al., 2001). In this earlier report, however, aPKC protein levels were not increased in pVHL-defective cells, leading the authors to speculate that pVHL targets a minor subpopulation of aPKC corresponding to the hyperphosphorylated, activated form of the enzyme. In support of this idea, we detected an increase in a slowly migrating form of aPKC in immunoblot assays of pVHL-defective cells (Figure 2D). This aPKC species is likely to be a phosphorylated, and hence presumably activated, form of aPKC because a single, faster migrating aPKC band was detected after treatment with lambda phosphatase (data not shown). Importantly, this slowly migrating aPKC species was suppressed by wild-type pVHL, but not type 2C pVHL mutants, and its abundance was mirrored by changes in aPKC kinase activity (Figure 2E). JunB, in contrast to HIF-2α and the AP-1 family member c-Jun, was also downregulated with a pharmacological aPKC inhibitor (Figure 2F and Figure S3). These results suggest that pVHL regulates JunB via both aPKC and HIF.

Loss of pVHL promotes neuronal survival

Pheochromocytoma cells are derived from sympathetic neuronal precursor cells, and PC12 rat pheochromocytoma cells, which are *VHL*$^{+/+}$, have been used as a model to study the regulation of neuronal survival by NGF. During normal neuronal development, many cells undergo apoptosis as they compete for NGF. Loss of NGF leads to activation of c-Jun and the induction of apoptosis (Ham et al., 1995; Palmada et al., 2002; Schlingensiepen et al., 1994; Xia et al., 1995). PC12 cells resemble differentiated sympathetic neurons when grown under low-serum conditions in the presence of NGF (Greene, 1978; Greene and Tischler, 1976) (Figure 3A). The nuclei of PC12 cells transfected to produce GFP-histone and induced to differentiate with NGF were uniform and intact. Consistent with earlier studies, NGF withdrawal led to morphological changes characteristic of apoptosis, including plasma membrane blebbing, cell body shrinkage, neurite retraction, and nuclear condensation and fragmentation (Deckwerth and Johnson, 1993; Edwards and Tolkovsky, 1994) (Figures 3A and 3B). The percentage of apoptotic cells at any time point is <20% with this experimental paradigm because PC12 cells do not die synchronously under these conditions (Francois et al., 2001; Messam and Pittman, 1998).

In addition to cell death, we observed that JunB is downregulated after NGF withdrawal from PC12 cells (Figure 3C). Since

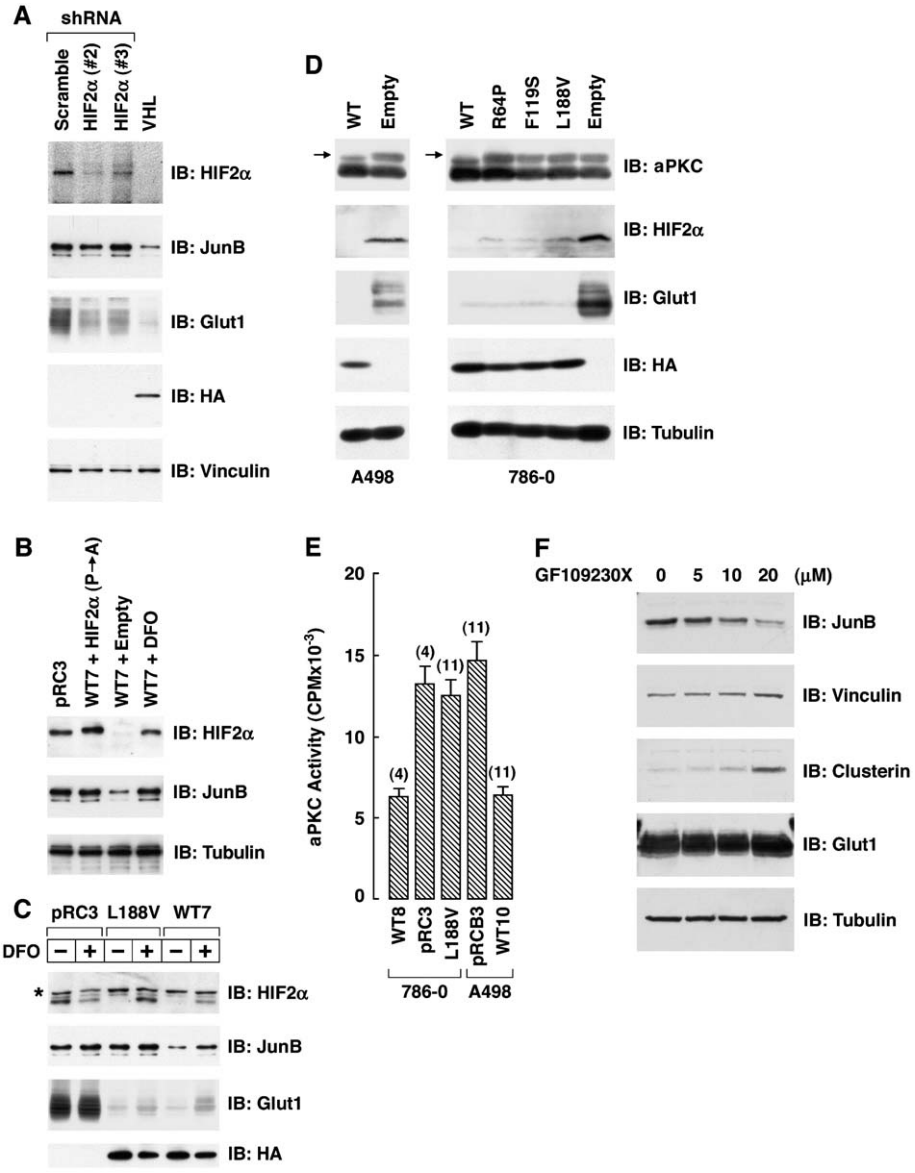

Figure 2. Regulation of JunB by pVHL involves HIF-dependent and HIF-independent pathways

A: Immunoblot analysis of 786-O *VHL*$^{-/-}$ renal carcinoma cells retrovirally infected to produce the indicated short hairpin RNAs (shRNA) or wild-type pVHL (VHL).

B: Immunoblot analysis of RC3 cells and WT7 cells. Where indicated, WT7 cells were treated with DFO or infected to produce HIF-2α P405A;P531A or with empty retrovirus.

C: Immunoblot analysis of indicated 786-O subclones grown in presence or absence of DFO. Asterisk indicates nonspecific band.

D: Immunoblot analysis of A498 and 786-O cells transfected to produce the indicated HA-pVHL variants or with empty vector. Arrow indicates a slowly migrating form of aPKC.

E: In vitro aPKC activity. Anti-aPKC immunoprecipitates of the indicated cell lines under antibody excess conditions were incubated with a peptidic aPKC substrate in the presence of ^{32}P-γ-ATP. Shown are incorporated ^{32}P values. Error bars = 1 standard deviation.

F: Immunoblot analysis of 786-O cells treated with the PKC inhibitor GF109230X.

JunB antagonizes c-Jun in many settings, we asked whether loss of pVHL or elevated JunB could block apoptosis after NGF withdrawal. In these experiments, PC12 cells were again transfected with a plasmid encoding GFP-histone to identify transfected cells and score apoptotic nuclei, in addition to the plasmid or siRNA of interest. After recovery from transfection, the cells were grown in the presence of NGF for 5–7 days and then placed in NGF-free media. Apoptosis was substantially reduced by JunB (Figure 4A and Figure S4). This effect was specific because it was not observed with a dimerization-defective JunB mutant. Likewise, JunB suppressed apoptosis of rat primary sympathetic neurons after NGF deprivation (Figure 4C). Treatment of PC12 with siRNA against rat VHL, but not various control siRNAs, also decreased apoptosis after NGF withdrawal (Figure 4B). This effect was specifically due to downregulation of pVHL because it was reversed by a plasmid encoding wild-type human pVHL. Importantly, the best-studied type 2C pVHL mutant, L188V, did not reverse the effects of the VHL siRNA (Figure 4B) despite its ability to downregulate HIF (Figure 2C). In contrast, the elongin binding mutant pVHL C162F, which is grossly defective with respect to HIF regulation (Ohh et al., 2000) (see also Figure 7E), was partially active in this assay. Collectively, these results implicate deregulation of JunB and escape from NGF-dependent apoptosis in the pathogenesis of VHL-associated pheochromocytoma. Similarly, an activated c-RET mutant linked to pheochromocytoma (C634R) and known to promote cell survival (De Vita et al., 2000), but not wild-type c-RET, induced JunB in PC12 cells and decreased apoptosis under NGF-poor conditions (Figures 4D and 4E).

Induction of neuronal apoptosis is a specific attribute of EglN3 and is hydroxylase dependent

We confirmed the earlier observations of others that EglN3, which in rat cells is called SM-20, is rapidly induced in PC12

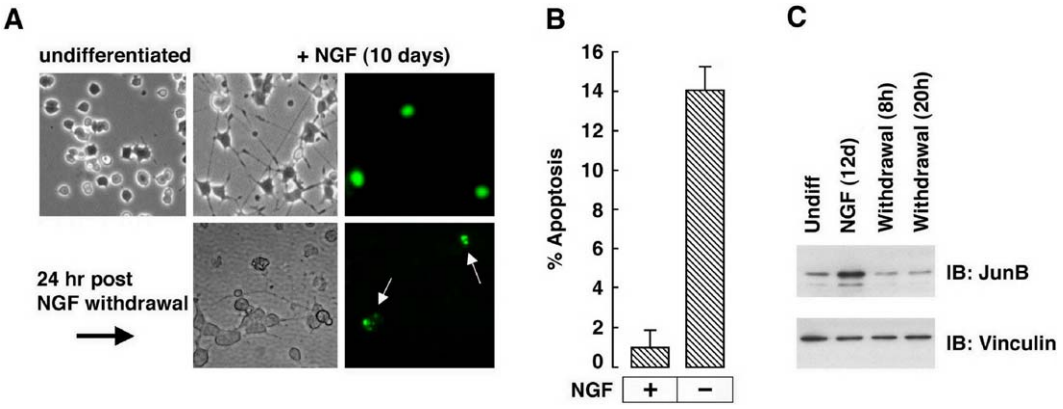

Figure 3. Apoptosis and increased JunB after NGF withdrawal

A and B: Phase-contrast and fluorescent photomicrographs of PC12 cells transfected to produce GFP-histone and grown in serum-rich media (undifferentiated) or serum-poor media supplemented with NGF for 10 days, which was then withdrawn for 24 hr. White arrows indicate apoptotic nuclei, which were quantitated in **B** as percentage of GFP-positive nuclei. Error bars = 1 standard deviation.

C: Immunoblot analysis of PC12 grown under serum-rich conditions (Undiff), under serum-poor conditions supplemented with NGF for 12 days, or after NGF withdrawal.

cells after NGF withdrawal and kills these cells when ectopically expressed (Lipscomb et al., 1999, 2001; Straub et al., 2003) (Figure 5A and data not shown). We next transfected undifferentiated PC12 cells with plasmids encoding hemagglutinin (HA)-tagged versions of EglN1, EglN2, or EglN3 along with the plasmid encoding GFP-histone. The nuclei of cells producing HA-EglN1 or HA-EglN2 appeared healthy 72 hr after transfection and were comparable to cells producing GFP-histone alone (Figures 5B and 5C). In contrast, the nuclei of 14%–20% of the cells producing HA-EglN3 displayed the hallmarks of apoptosis 48–72 hr after transfection. The fact that <20% of the cells appeared apoptotic at any point in time is reminiscent of the asynchronous cell death observed after NGF withdrawal (Francois et al., 2001; Messam and Pittman, 1998). Increased apoptosis was not observed in cells producing an EglN3 variant in which a canonical histidine residue important for hydroxylase activity was converted to alanine (H196A) (Figures 5B and 5C and Figure S5). Comparable amounts of the different EglN species were produced in these experiments as determined by anti-HA immunoblot analysis (Figure 5D). Therefore, induction of neuronal apoptosis is specific to EglN3 among the EglN family members and requires its enzymatic activity. *C. elegans* have a single EglN gene called *Egl-9* (Epstein et al., 2001; Taylor, 2001). A role for EglN in neuronal apoptosis is supported by the observation that *Egl-9*$^{-/-}$ worms are resistant to certain neurotoxins (Darby et al., 1999).

EglN1, and not EglN3, appears to be the primary HIF prolyl hydroxylase under normal conditions in cells (Berra et al., 2003; A. Bommi-Reddy and W.G. Kaelin, unpublished data). Moreover, EglN3-induced apoptosis was not diminished when PC12 cells were cotransfected to produce HIF-1α or HIF-2α variants that can not be hydroxylated on proline (Figure S6). Collectively, these results suggest that HIF-α is not the relevant target of EglN3 in this system.

Transfection of PC12 cells with SM-20 siRNAs, but not various irrelevant or scrambled siRNAs, prior to differentiation and NGF withdrawal substantially decreased apoptosis (Figures 5E and 5F and Figure S7), indicating that EglN3/SM-20 hydroxylase is necessary, as well as sufficient, for the induction of apoptosis by NGF withdrawal. Accordingly, apoptosis after NGF withdrawal was also decreased under low-oxygen conditions or in the presence of cobalt chloride, both of which inhibit hydroxylase activity (Figures 5G and 5H).

SDH activity is required for EglN3/SM-20-induced neuronal apoptosis

Prolyl hydroxylation by EglN family members, which belong to a superfamily of 2-oxoglutarate (2-OG)-dependent dioxygenases, is coupled to conversion of 2-OG into succinate (Aravind and Koonin, 2001; Gunzler and Weidmann, 1998; Schofield and Zhang, 1999). SDH is an inner mitochondrial membrane enzyme that oxidizes succinate into fumarate as part of the Krebs cycle and also participates in electron transport. Two predictable outcomes of SDH inactivation would be the accumulation of succinate, which feedback inhibits 2-OG-dependent dioxygenases such as collagen prolyl hydroxylase and thymine-7-hydroxylase in vitro (Holme, 1975; Myllyla et al., 1977), and increased production of reactive oxygen species (Lenaz et al., 2004; McLennan and Degli Esposti, 2000; Yankovskaya et al., 2003), which can inhibit EglN activity (Gerald et al., 2004). To test whether succinate can also inhibit EglN3 prolyl hydroxylase activity, we exploited the fact that EglN3 can hydroxylate a HIF-1α-derived peptide in vitro, as determined by capture of ^{35}S-labeled pVHL (Bruick and McKnight, 2001; Epstein et al., 2001). As predicted, EglN3 hydroxylase activity was diminished in the face of increasing amounts of succinate (Figure 6A). Hydroxylation activity was restored, however, by the addition of 2-OG (Figure 6A), indicating that succinate and 2-OG act competitively in vitro. Intracellular succinate levels can approach 0.5 mM and are in vast excess of 2-OG following SDH inhibition (Selak et al., 2005). In addition, we confirmed that ROS production was increased in PC12 cells treated with pharmacological SDH inhibitors (Figure 6B), consistent with findings obtained with cells expressing a mutated form of SDHC (Ishii et al., 2005).

Motivated by these findings, we asked whether SDH activity

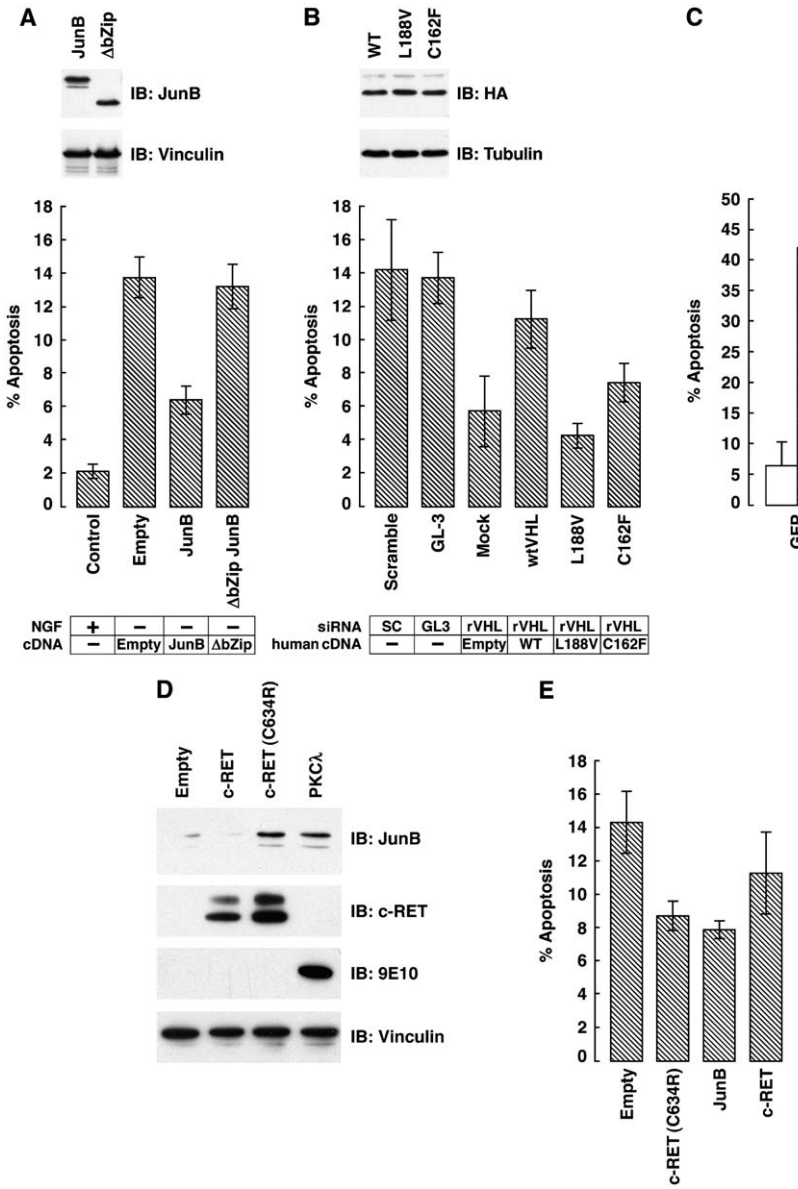

Figure 4. JunB blunts apoptosis after NGF withdrawal

A and E: PC12 cells were transfected with a plasmid encoding GFP-histone along with plasmid encoding wild-type JunB, dimerization-defective JunB (ΔbZip), c-RET, or the backbone plasmid (Empty). Shown is the percentage of GFP-positive nuclei exhibiting apoptotic changes after growth in NGF for 5–7 days followed by NGF withdrawal (−). Control, cells transfected with GFP-His alone and maintained in NGF (+). **B:** PC12 cells were transfected with a plasmid encoding GFP-histone along with siRNA against rat VHL (rVHL) and a plasmid encoding the indicated human pVHL variants. Where indicated, rVHL siRNA was replaced with scrambled (SC) or luciferase (GL3) siRNA. Shown is the percentage of GFP-positive nuclei exhibiting apoptotic changes after growth in NGF for 5–7 days followed by NGF withdrawal. **C:** Primary sympathetic neurons were electroporated to produce GFP alone (GFP) or GFP and Myc-tagged JunB (JunB) and treated with NGF for 3 days. Shown is the percentage of GFP-positive cells with apoptotic nuclei after continued NGF treatment (open bars) or 48 hr after NGF withdrawal (hatched bars). **D:** Immunoblot of PC12 cells transfected to produce the indicated c-RET proteins or Myc-tagged PKC-λ and grown in the absence of NGF. Error bars = 1 standard deviation.

influences EglN3-induced apoptosis by cotransfecting undifferentiated PC12 cells with plasmids encoding HA-EglN3 and GFP-histone in the presence or absence of pharmacological SDH inhibitors. Three different inhibitors, malonic acid (MA), 3-nitroproprionic acid (3-NPA), and thenoyl trifluoroacetone (TTFA), decreased EglN3-induced apoptosis (Figures 6C and 6D). Notably, HIF-α protein levels were not increased by these agents, in contrast to PC12 cells treated with the hypoxia-mimetic cobalt chloride, which further argues that EglN3-induced neuronal apoptosis is HIF-α independent (Figure 6E). Coadministration of the antioxidant ascorbic failed to mitigate the effects of the SDH inhibitors on EglN3-induced apoptosis despite blocking ROS induction (Figures 6B and 6F), suggesting that a non-ROS mechanism such as succinate accumulation attenuates EglN3-induced apoptosis when SDH activity is impaired.

To assess the role of SDH in neuronal apoptosis in a more physiological context, we next transfected PC12 cells with the GFP-histone plasmid along with siRNAs prior to NGF treatment and withdrawal. Two different SDHD siRNAs, but not various control siRNAs, dramatically decreased apoptosis after NGF withdrawal (Figure 6G and Figures S8 and S9). Notably, apoptosis was partially restored in this setting by the addition of 2-OG to the media (Figure 6G). The SDH inhibitors (MA or 3-NPA) also diminished apoptosis in this setting (Figure S10). Taken together, these findings suggest that inactivation of SDH, by promoting the accumulation of succinate, impairs EglN3-induced apoptosis and promotes survival when NGF levels become limiting.

c-Jun acts upstream of SM-20/EglN3 in the NGF signaling pathway

We next asked if SM-20/EglN3 and c-Jun function in the same pathway. Apoptosis induced by overexpression of EglN3 in

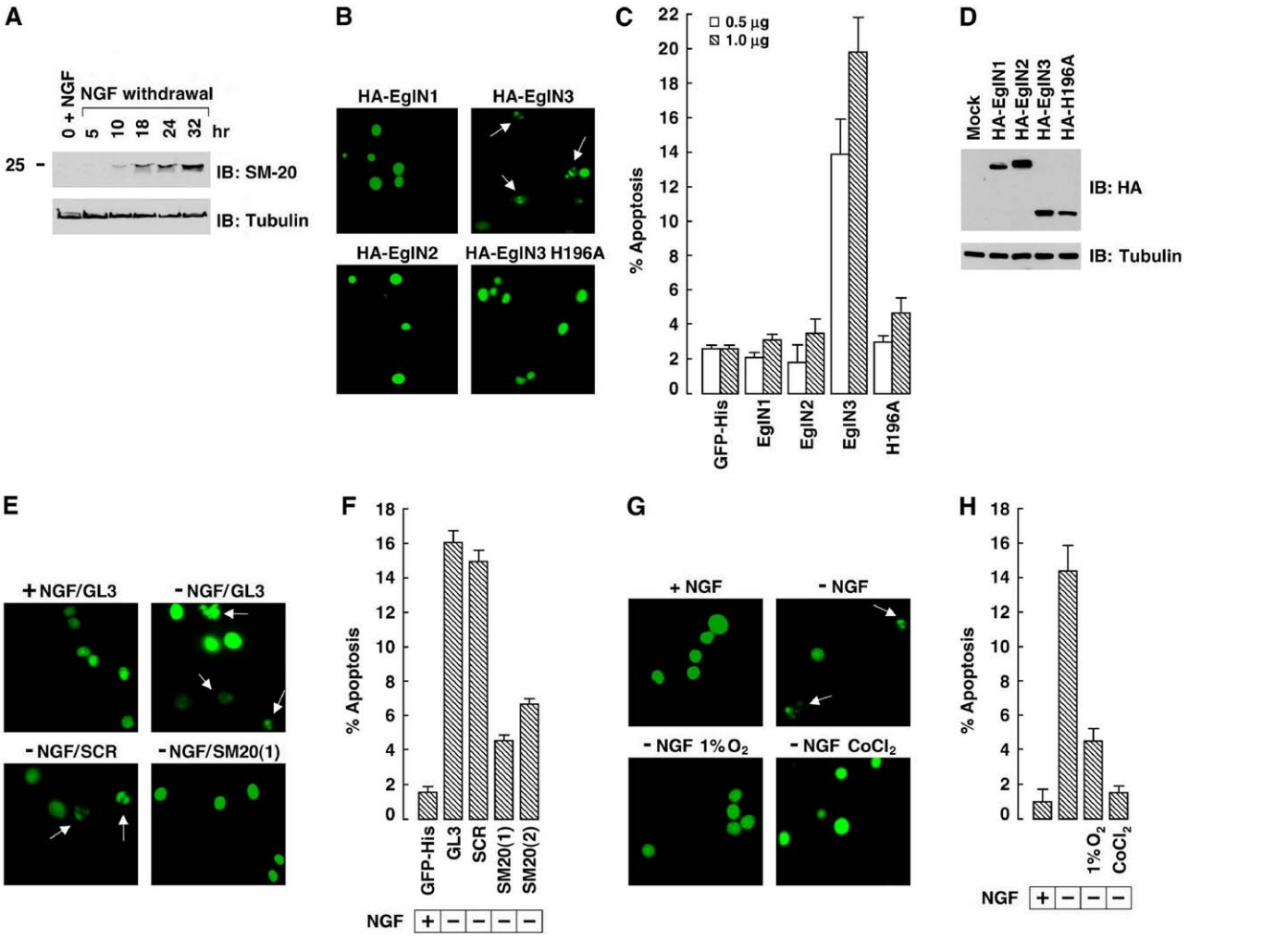

Figure 5. EglN3 is sufficient and necessary for induction of apoptosis by NGF withdrawal

A: Anti-SM-20/EglN3 immunoblot analysis of PC12 cells treated as in Figure 3A. **B and D:** Representative fluorescent photomicrographs (**B**) and anti-HA immunoblot analysis (**D**) of PC12 cells transfected to produce GFP-histone and the indicated HA-EglN species. White arrows in **A** indicate apoptotic nuclei. **C:** Percentage of GFP-positive nuclei with apoptotic changes after transfection with 0.5 or 1.0 μg of the indicated plasmids. **E and F:** Representative fluorescent photomicrographs of PC12 cells transfected with the indicated siRNAs and a plasmid encoding GFP-histone followed by treatment with NGF for 10 days (+NGF), which was then withdrawn for 24 hr (−NGF). White arrows indicate apoptotic nuclei, which were quantitated in **E** as percentage of GFP-positive nuclei. **G and H:** Representative fluorescent photomicrographs (**G**) of PC12 cells transfected to produce GFP-histone and treated with NGF for 5 days (+NGF), which was then withdrawn for 24 hr (−NGF). Where indicated, cells were exposed to 100 μM $CoCl_2$ or 1% hypoxia during NGF withdrawal. White arrows indicate apoptotic nuclei, which were quantitated in **H** as percentage of GFP-positive nuclei. Error bars = 1 standard deviation.

PC12 cells, in contrast to that induced by NGF withdrawal, was not reduced by coexpression of the c-Jun antagonist JunB (Figure 7A). In a reciprocal set of experiments, PC12 cells were cotransfected with plasmids encoding an activated, stabilized version of c-Jun (Δc-Jun) and GFP-histone. Inclusion of SM-20 siRNAs, but not control siRNAs, in the transfection mix dramatically reduced c-Jun-dependent apoptosis, arguing that SM-20/EglN3 acts downstream of or parallel to c-Jun (Figure 7B). In support of the former possibility, wild-type, but not mutant, c-Jun activated a luciferase reporter plasmid containing the SM-20 promoter in cotransfection assays (Figure 7C), and SM-20 levels increased in PC12 cells infected with an adenovirus encoding c-Jun (Figure 7D).

EglN3 is induced by NGF withdrawal but also by HIF (Aprelikova et al., 2004; Cioffi et al., 2003; del Peso et al., 2003; Marxsen et al., 2004). Therefore, pVHL has opposing effects on EglN3, and the balance of those effects might dictate the risk of developing pheochromocytoma. In support of this, we detected high basal EglN3 mRNA and protein levels in 786-O cells producing type 1 pVHL mutants (as well as in 786-O cells stably transfected with an empty vector), which are associated with a low risk of pheochromocytoma, and low EglN3 levels in 786-O cells producing type 2 pVHL mutants, which are associated with a high risk of pheochromocytoma (Figures 7E and 7F). We do not currently understand why EglN3 levels are low in cells producing type 2A and type 2B pVHL mutants, however, since the HIF and JunB levels in these cells are comparable to those observed in cells producing type 1 pVHL mutants (Figure 7E and Figure S11). Gene expression profiling indicates that a subset of HIF target genes, including EglN3, are inhibited by type 2 pVHL mutants despite increased HIF levels (data not shown). This might reflect a residual physical interaction be-

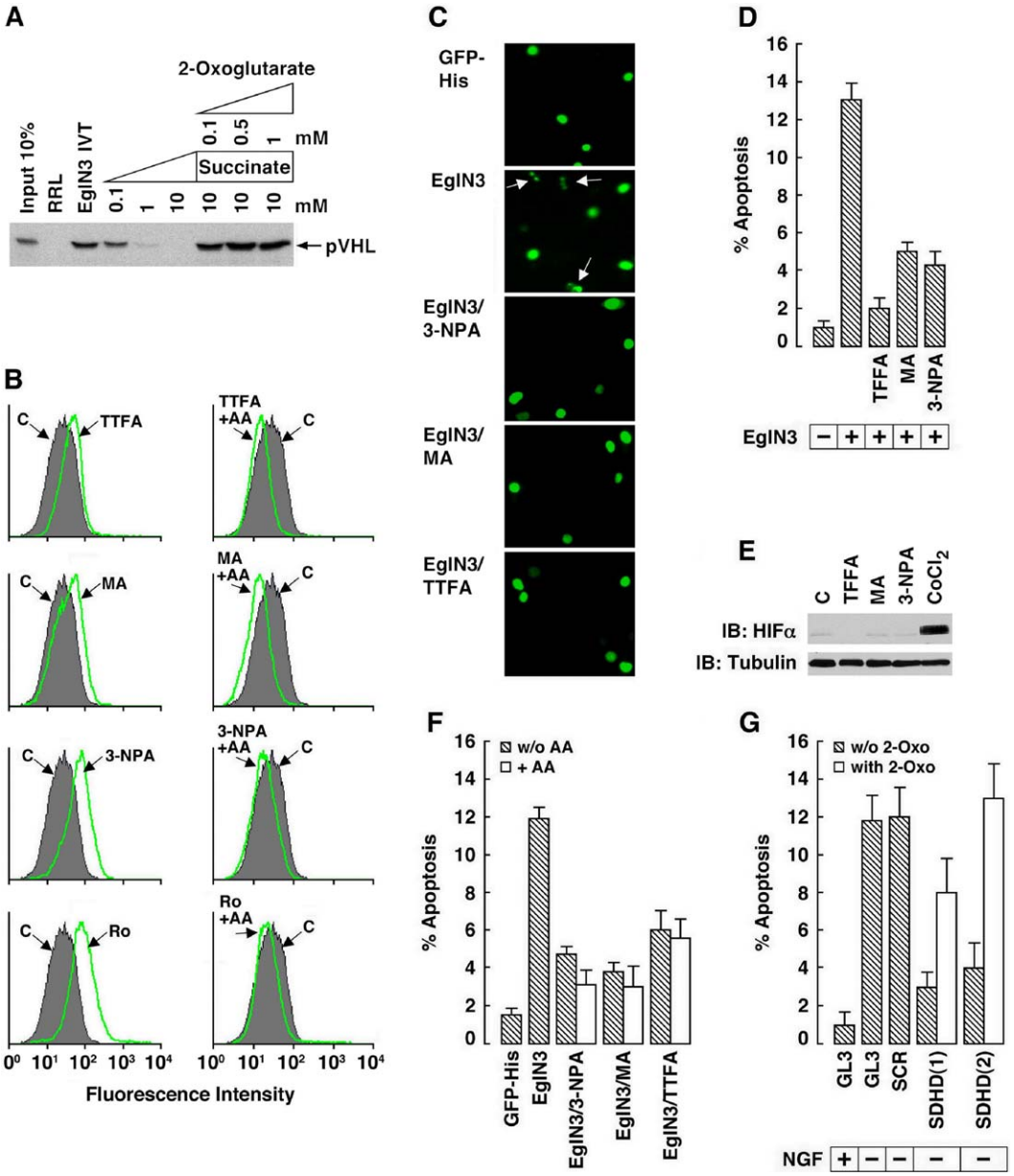

Figure 6. SDH activity is required for EglN3-induced apoptosis

A: Binding of ^{35}S-labeled pVHL to biotinylated HIF-1α peptide after preincubation with unprogrammed reticulocyte lysate (RRL), EglN3 in vitro translate (EglN3 IVT), or EglN3 IVT with the indicated concentrations of succinate and 2-oxoglutarate. ^{35}S-pVHL was loaded directly in lane 1 as a control.

B: FACS profiles of PC12 cells stained with the ROS-sensitive dye CM-H2DCFDA after treatment with the indicated SDH inhibitors or the ROS-inducing agent rotenone (Ro; 20 μM) in the presence or absence of the ROS scavenger ascorbic acid (AA; 100 μM). C, control.

C and D: Representative fluorescent photomicrographs of PC12 cells (**C**) transfected to produce GFP-histone alone (GFP-His) or GFP-histone and EglN3 (EglN3). The SDH inhibitors 3-NPA (300 μM), MA (300 μM), or TTFA (200 μM) were added where indicated. White arrows indicate apoptotic nuclei, which were quantitated in **D** as percentage of GFP-positive nuclei.

E: Immunoblot analysis of PC12 cells treated with the indicated chemicals or vehicle (**C**).

F: Percentage of GFP-positive PC12 nuclei undergoing apoptosis after transfection to produce GFP-histone alone (GFP-His) or GFP-histone and EglN3 (EglN3) in the presence or absence of SDH inhibitors. One hundred micromolar AA was also present where indicated.

G: Percentage of GFP-positive PC12 nuclei undergoing apoptosis after transfection with the indicated siRNAs and a plasmid encoding GFP-histone followed by treatment with NGF for 5 days (+NGF), which was then withdrawn for 24 hr (−NGF). Where indicated, 0.5 mM 2-oxoglutarate was added to the media 24 hr before NGF withdrawal.

Error bars = 1 standard deviation.

tween pVHL and HIF that affects HIF function rather than HIF stability. Alternatively, it might reflect a pVHL activity directed against a protein that cooperates with HIF to activate transcription.

Discussion

We discovered that inactivation of pVHL leads to increased levels of JunB and that induction of JunB in this setting reflects

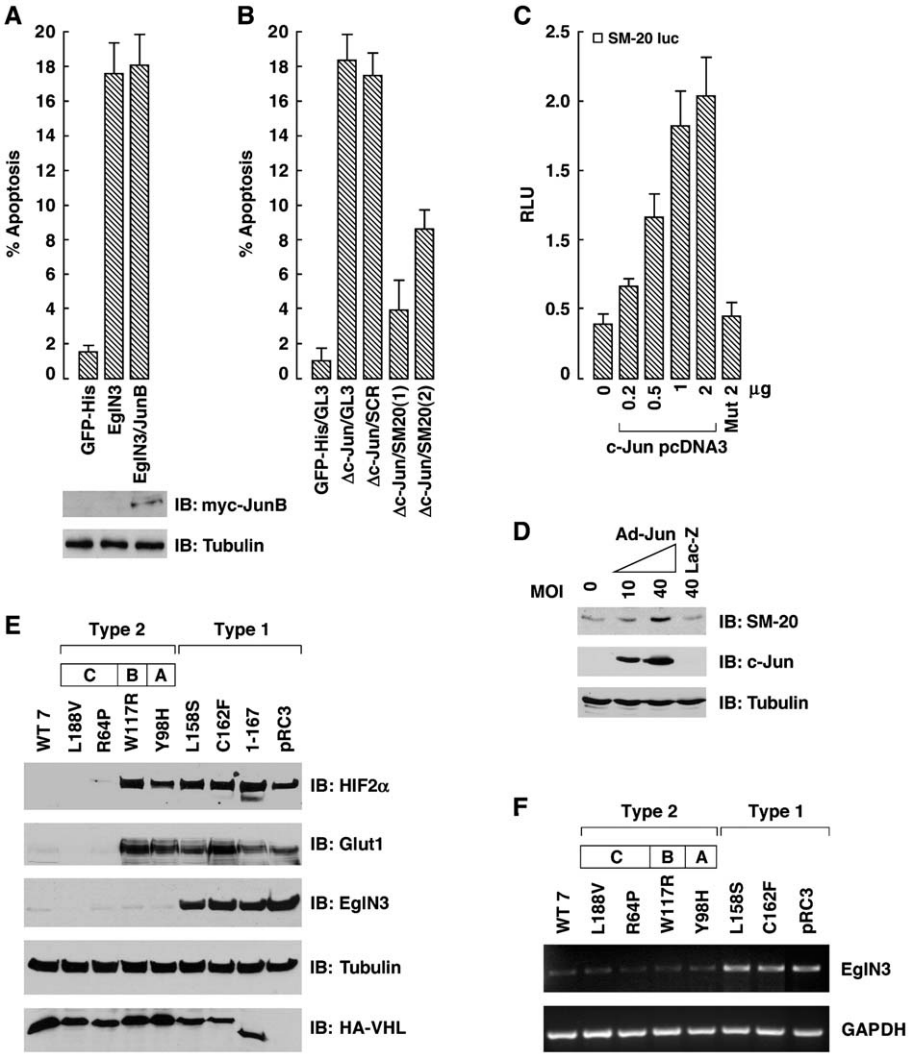

Figure 7. EglN3 activity is required for Jun-induced apoptosis

A: Percentage of GFP-positive PC12 nuclei undergoing apoptosis transfected to produce GFP-histone alone (GFP-His) or GFP-histone and EglN3 (EglN3) with or without Myc-tagged JunB.

B: Percentage of GFP-positive PC12 nuclei undergoing apoptosis transfected with plasmids encoding GFP-histone alone (GFP-His) or GFP-histone and activated c-Jun (Δc-Jun) along with the indicated siRNAs.

C: Normalized luciferase values of PC12 cells transfected with reporter plasmid containing firefly luciferase under the control of SM-20 promoter and plasmid encoding wild-type or mutant (DNA binding-defective) c-Jun.

D: Immunoblot analysis of PC12 cells infected with adenovirus encoding c-Jun or β-galactosidase at indicated multiplicity of infection (MOI).

E and F: Immunoblot (**E**) and semiquantitative RT-PCR analysis (**F**) of 786-O cells stably transfected to produce the indicated pVHL species. Error bars = 1 standard deviation.

both increased aPKC activity and increased HIF levels. Every disease-associated pVHL mutant tested so far, including familial pheochromocytoma pVHL mutants that retain the ability to degrade HIF, fails to downregulate JunB. JunB can antagonize c-Jun in certain settings. Increased JunB levels attenuate the induction of apoptosis in pheochromocytoma cells after NGF withdrawal, which is mediated by c-Jun. Another protein suspected of playing a role in apoptosis following NGF withdrawal is EglN3. We found that EglN3 is both necessary and sufficient for the induction of apoptosis after NGF withdrawal and is unique among the three EglN family members in this regard. Moreover, EglN3 appears to act downstream of c-Jun and is sensitive to changes in SDH activity.

Our findings solidify the role of pVHL in the regulation of aPKC (Okuda et al., 1999, 2001; Pal et al., 1997) and place this regulation in a physiological context. Earlier studies showed that aPKC is activated by NGF (Vandenplas et al., 2002; Wooten et al., 2001), which regulates both c-Jun and JunB. pVHL antagonizes activated aPKC and thereby attenuates NGF signaling.

Our findings provide mechanistic links between SDH mutations, EglN3 activity, and escape from neuronal apoptosis. Inhibition of EglN3 after SDH inactivation appears to be due to the accumulation of succinate, which can be transported to the cytosol by the dicarboxylate carrier located on the inner mitochondrial membrane. Additional studies will be required to determine the ratios of succinate/2-OG achieved in specific subcellular compartments when SDH activity is impaired. This information, along with differences in subcellular localization (Metzen et al., 2003) and sensitivity to 2-OG analogs (Hirsila et al., 2003) among the EglN paralogs, might explain our failure to detect accumulation of the EglN1 target HIF-α following SDH inactivation in PC12 cells as well as in many other cell types (data not shown). This, as well as other lines of evidence presented here, strongly suggests that HIF is not the relevant target of SDH and EglN3 with respect to neuronal apoptosis. Nonetheless, our data do not preclude the possibility that SDH inactivation also affects EglN1 and HIF, especially after prolonged SDH inactivation or in susceptible cell types. For example, increased HIF activity has been observed in 293T human embryonic kidney cells treated with SDH inhibitors (Selak et al., 2005), in pheochromocytomas linked to SDH mutations (Gi-

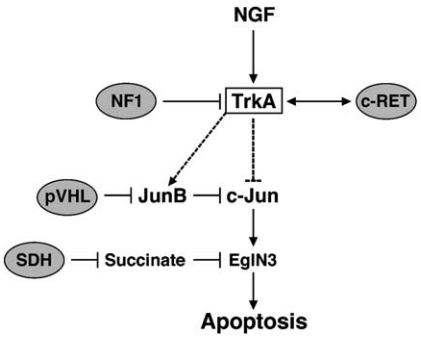

Figure 8. Model linking familial pheochromocytoma genes to apoptosis after NGF withdrawal

menez-Roqueplo et al., 2001), and in papillary renal cancers linked to mutations in fumarate hydratase (FH), which acts downstream of SDH (Isaacs et al., 2005).

Germline mutations in either *NF1*, *c-RET*, *SDH*, or *VHL* cause familial pheochromocytoma and the related tumor, paraganglioma (Bryant et al., 2003; Maher and Eng, 2002). Based on our studies, we propose that deregulation of NGF signaling is the relevant unifying feature of these mutations (Figure 8). NF1 inhibits downstream signaling by NGF receptor TrkA. Accordingly, loss of NF1 promotes NGF-independent survival of embryonic peripheral neurons (Vogel et al., 1995). c-RET is the receptor for GDNF (glial cell line-derived neurotrophic factor) and can crosstalk with the NGF receptor TrkA (Dechant, 2002; Peterson and Bogenmann, 2004; Tsui-Pierchala et al., 2002). We found that activation of c-RET, like loss of pVHL, leads to the induction of JunB and attenuates apoptosis after NGF withdrawal. Finally, SDH inactivation blunts neuronal apoptosis through its effects on EglN3. We propose that mutations in these genes cause pheochromocytoma because certain neuronal precursor cells with the capability of forming pheochromocytomas are not properly culled during development. Mutation of these genes would no longer be detrimental, however, once this developmental window had passed. This model would explain why somatic *NF1*, *c-RET*, *SDH*, and *VHL* are extremely rare in nonhereditary pheochromocytomas (Maher and Eng, 2002) and are mutually exclusive. At the same time, ~25% of seemingly sporadic pheochromocytomas are due to previously unsuspected germline mutations in one of these four genes (Neumann et al., 2002).

Abnormal NGF signaling has been linked to other cancers, including the pediatric tumors neuroblastoma and medulloblastoma (Katsetos et al., 2003; Nakagawara, 2001). It is tempting to speculate that alterations in developmental apoptosis play a role in these tumors also, especially in light of the spontaneous regressions that sometimes occur in neuroblastoma patients who present within the first year of life. Neuroblastoma, like pheochromocytoma, is derived from neural crest progenitor cells that give rise to the sympathetic nervous system, adrenal medulla, and adrenergic and cholinergic neuroblasts along the sympathetic chain and cranial ganglia. Our findings might also be relevant to the earlier observation that pVHL can transform neuroblastoma cells into functional neuron-like cells (Murata et al., 2002).

In summary, we propose that germline *NF1*, *c-RET*, *SDH*, and *VHL* mutations allow sympathetic neuronal progenitors to escape from developmental apoptosis and thereby set the stage for their neoplastic transformation. In contrast, somatic mutations in these genes in the adult would not predispose to pheochromocytoma, in keeping with molecular epidemiological data. It is possible that escape from developmental apoptosis plays a role in pediatric cancers and other forms of hereditary cancer as well.

Experimental procedures

Cell lines

The 786-O and A498 renal carcinoma cell line derivatives are described elsewhere (Kondo et al., 2003; Lonergan et al., 1998) and were maintained in Dulbecco's modified Eagle's medium (DMEM) containing 10% fetal clone (Hyclone) and, where appropriate, G418 and/or puromycin, in the presence of 10% CO_2 at 37°C. Undifferentiated PC12 cells were maintained in DMEM containing 10% fetal bovine serum (Hyclone) and 5% horse serum (Sigma) in 37°C, 10% CO_2 incubator.

Plasmids

The human JunB open reading frame cDNA in a Gateway entry plasmid (a gift of Marc Vidal) was transferred to the Gateway expression vector pDEST47 (Invitrogen) by recombination cloning to make pDEST47-JunB. The JunB cDNA was PCR amplified with primer A (5′-GGGGACAAGTTTGTACAAAAAAGCAGGCTATGTGCACTAAAATGGAACAGCCCT-3′) and primer B (5′-GGGGACCACTTTGTACAAGAAAGCTGGGTCCTAGCGCGCGATGCGCTCCAGCTT-3′) to make the JunBΔbZip cDNA, which was transferred to pDEST47 by sequential BP and LR recombination reactions according to the manufacturer's instructions (Invitrogen). The human c-RET cDNA, encoding the short 1072 residue c-RET isoform, in a Gateway entry plasmid (a gift of Marc Vidal), was similarly transferred to pDEST47 (Invitrogen) by recombination cloning to make pDEST47-c-RET. The c-RET cDNA was PCR amplified with primer C (5′-CCACTGTGCGACGAGCTGCGCCGCACGGTGATCGCAGCC-3′) and primer D (5′-GGCTGCGATCACCGTGCGGCGCAGCTCGTCGCACAGTGG-3′) to make the constitutively active C634R c-RET mutant, which was also transferred to pDEST47.

The pVHL expression plasmids have been described before (Hoffman et al., 2001).

The expression plasmids for HA-EglN1 (Ivan et al., 2002) and HA-HIF-2α P405A;P531A (Kondo et al., 2003) were described previously, and the plasmids for HA-EglN2, HA-EglN3, and HA-HIF-1α P402A;P564A were made analogously. HA-EglN3 H196A was made using a site-directed mutagenesis kit (GeneEditor; Promega). The pcDNA-Myc-JunB was made by PCR amplification of IMAGE-clone MGC 10557 with primers that introduced a 5′ BamH1 site and 3′ EcoR1 site followed by ligation into 5x-myc-pcDNA3. The plasmid encoding human Δc-Jun, which harbors mutations analogous to the chicken v-Jun mutations, was described before (Wei et al., 2005). To make the c-Jun leucine zipper mutant, a c-Jun cDNA corresponding to residues 1–255 was amplified by PCR with primers that introduced a 5′ BamHI site and 3′ EcoRI site and ligated into 5x-myc-pcDNA3. All cDNAs were sequence verified.

EMSA

Synthetic oligonucleotides were end labeled with [γ^{32}P]-ATP and T4 DNA Kinase (New England Biolabs) according to the manufacturer's instructions and annealed in vitro for use in EMSA containing 5 μg of nuclear extract (9 μg for supershift assays), prepared using a Nuclear Extract Kit (Active Motif), in a final volume of 20 μl in the presence of 10 mM Tris-HCl (pH 7.5), 50 mM NaCl, 1 mM EDTA, 10% glycerol, 1 mM DTT, and 2 μg of poly (dI-dC). The clusterin promoter-derived EMSA probe sequences (sense strands) were as follows: wild-type, 5′-TTCTTTGGGCGTGAGTCATGCA-3′; ΔAP-1, 5′-TTCTTTGGGCGTGAGGCATGCA-3′; ΔSp1, 5′-TTCTTTGTTCGTGAGTCATGCA-3′. Canonical binding site probe sequences (sense) were as follows: Sp1, 5′-ATTCGATCGGGGCGGGGCGAGC-3′; and AP-1, 5′-CGCTTGATGAGTCAGCCGGAA-3′. Competitor unlabeled probes were annealed in vitro and used at 50-fold molar excess of labeled probe. Supershift assays were performed with polyclonal anti-JunB Nushift Antibody (Active Motif) and Nushift Kit (Active Motif) according to the manufacturer's instructions. Differential supershifts were not observed with antisera against c-Fos or c-Jun (data not shown).

Immunoblot analysis

Twenty micrograms of nuclear extract per lane, prepared using a NE-PER extraction kit (Pierce) and measured by the Bradford assay, was resolved on 10% or 12% SDS-PAGE gels and transferred to nitrocellulose membrane (Bio-Rad) to detect endogenous JunB and HIF-2α. After blocking in TBS with 5% nonfat milk, the membranes were probed with anti-JunB monoclonal antibody (C-11; Santa Cruz Biotechnology) or anti-HIF-2α rabbit polyclonal antibody (NB100-122; Novus Biologicals). Bound protein was detected with horseradish peroxidase (HRP)-conjugated secondary antibodies and an enhanced chemiluminescence kit (Pierce).

HA-EglN1, HA-EglN2, HA-EglN3, HA-H196A, and HA-HIF-2α were detected in whole-cell extracts using polyclonal α-HA (Y-11; Santa Cruz). HA-HIF-1α was detected using monoclonal anti-HIF-1α (Transduction Lab). The antibody against EglN3/SM-20 was a gift of Peter Ratcliffe and was described previously (Appelhoff et al., 2004). The antibody against rodent HIF-1α, which also recognizes HIF-2α (data not shown), was a gift of Jacques Pousegeur and was described in Berra et al. (2003).

siRNA

Short interfering RNA (siRNA) oligonucleotides were purchased from Dharmacon. Sense strand sequences were as follows: rVHL, 5′-AAUGUUGAUGGACAGCCUAUU-3′; hVHL #7, 5′-AAUGUUGACGGACAGCCUAUU-3′; GL3, 5′-CUUACGCUGAGUACUUCGAUU-3′; scramble, 5′-AACAGUCGCGUUUGCGACUGG-3′; SM-20 #1, 5′-CAGGUUAUGUUCGUCAUGUdTdT-3′; SM-20 #2, 5′-UUCUCCUGGUCAGACCGCAdTdT-3′; SDHD #1, 5′-GUUGCCAUGCUGUGGAAGCdTdT-3′; SDHD #2, 5′-UUGGACAAGUGGUUACUGAdTdT-3′.

In vitro kinase assays

In vitro kinase assays were performed as described elsewhere (Standaert et al., 2004) using a rabbit polyclonal antibody that recognizes the C termini of both PKC-λ and PKC-ζ (Santa Cruz Biotechnologies). Immunoprecipitates were incubated for 8 min at 30°C in 100 μl buffer containing 50 mM Tris/HCl (pH 7.5), 100 μM Na_3VO_4, 100 μM $Na_4P_2O_7$, 1 mM NaF, 100 μM PMSF, 4 μg phosphatidylserine (Sigma), 50 μM [γ-^{32}P]ATP (NEN Life Science Products), 5 mM $MgCl_2$, and as substrate, 40 μM serine analog of the PKC-ε pseudosubstrate (BioSource). After incubation, ^{32}P-labeled substrate was trapped on P-81 filter papers and counted.

Apoptosis assays

Undifferentiated PC12 cells were plated onto collagen-coated 6-well plates 1 day before transfection with Lipofectamine 2000 (Invitrogen) according to the manufacturer's instructions. Transfection mixes contained 500 ng of a plasmid encoding GFP-histone (a gift of Geoffrey Wahl), 1 μg of the cDNA expression plasmid of interest, and where indicated, 100 nM of siRNA. Forty-eight hours later, the cells were trypsinized, transferred to collagen-coated p100 dishes, and grown in DMEM supplemented with 1% horse serum and NGF (50 ng/ml) for 5–7 days. For NGF withdrawal, cells were washed once with serum-free medium followed by incubation in NGF-free medium containing a neutralizing antibody against the 2.5S and 7S forms of NGF (Accurate Chemical) at a 1:400 dilution. Control cells were washed once in NGF-free medium and then returned to NGF-containing medium. Nuclei that were condensed or fragmented were scored as apoptotic. Approximately 400 cells were scored for each set of conditions, and all assays were performed in triplicate.

Isolation of primary sympathetic neurons

Sympathetic neurons were isolated from the superior cervical ganglia (SCG) as previously described (Palmada et al., 2002). Briefly, SCG from Sprague-Dawley rats were isolated at postnatal day 4, and sympathetic neurons were dissociated with 0.25% trypsin and 0.3% collagenase for 30 min at 37°C. After dissociation, the neurons were electroporated with pmax-GFP alone (Amaxa) or pmax-GFP along with JunB expression plasmid according to the manufacturer's instructions (Amaxa Rat Neuron Nucleofector kit). The neurons were then cultured on poly-L-ornithine and laminin-coated 4-well slides (Nalge Nunc International) in Ultraculture medium (BioWhittaker) supplemented with 3% fetal calf serum (Gibco), 2 mM L-glutamine (Gibco), and 20 ng/ml NGF (Harlan). The neurons were maintained for 3 days in the presence of NGF and then washed twice in Ultraculture medium lacking NGF and once with Ultraculture containing an antibody to NGF at 0.1 μg/ml (Chemicon International), and returned to NGF-free media. The cells were fixed in paraformaldehyde 48 hr later, and the number of GFP-positive neurons with apoptotic nuclei, identified by DAPI staining (Vector Labs), were counted. At least 75 neurons were evaluated for each condition.

Hydroxylation assays

Hydroxylation assays were performed essentially as described before (Ivan et al., 2002).

ROS analysis

PC12 cells were incubated for 1 hr with 5 μM CM-H_2DCFDA (Molecular Probes), harvested, resuspended at 10^6 cells/ml in PBS supplemented with 7% FBS, and analyzed by FACS.

Luciferase assays

The HRE reporter was described in Kondo et al. (2002). The SM-20 promoter reporter was described in Menzies et al. (2004). Luciferase assays were performed in triplicate using a luciferase dual reporter assay system (Promega).

Adenovirus

The adenovirus encoding c-Jun was described earlier (Yu et al., 2001) and was a gift of Dr. Jason X.-J. Yuan.

Semiquantitative RT-PCR

Total RNAs were extracted with RNeasy Mini Kit (Qiagen). cDNA synthesis and PCR amplification were performed with Superscript One-Step RT-PCR (Invitrogen) using 1 μg total RNA. EglN3 cDNA was amplified with sense primer (5′-GCGTCTCCAAGCGACA-3′) and antisense primer (5′-GTCTTCAGTGAGGGCAGA-3′) for 32 cycles. As a control, GAPDH cDNA was also amplified with sense primer (5′-CTACACTGAGCACCAGGTGGTCTC-3′) and antisense primer (5′-GATGGATACATGACAAGGTGCGGC-3′). Ten microliter aliquots of the PCR reaction (50 μl) were separated on a 2% agarose gel.

Supplemental data

The Supplemental Data include eleven supplemental figures and can be found with this article online at http://www.cancercell.org/cgi/content/full/8/2/155/DC1/.

Acknowledgments

We thank Jacques Pousegeur, Peter Ratcliffe, Marc Vidal, and Jason X.-J. Yuan for valuable reagents; Hiroaki Kawanishi and Yasuo Awakura for help with real-time PCR assays; and members of the Kaelin Laboratory for useful discussions. Supported by grants from NIH and Murray Foundation. W.G.K. is a HHMI Investigator.

Received: February 5, 2005
Revised: April 29, 2005
Accepted: June 7, 2005
Published: August 15, 2005

References

Appelhoff, R.J., Tian, Y.M., Raval, R.R., Turley, H., Harris, A.L., Pugh, C.W., Ratcliffe, P.J., and Gleadle, J.M. (2004). Differential function of the prolyl hydroxylases PHD1, PHD2, and PHD3 in the regulation of hypoxia-inducible factor. J. Biol. Chem. *279*, 38458–38465.

Aprelikova, O., Chandramouli, G.V., Wood, M., Vasselli, J.R., Riss, J., Maranchie, J.K., Linehan, W.M., and Barrett, J.C. (2004). Regulation of HIF prolyl hydroxylases by hypoxia-inducible factors. J. Cell. Biochem. *92*, 491–501.

Aravind, L., and Koonin, E.V. (2001). The DNA-repair protein AlkB, EGL-9, and leprecan define new families of 2-oxoglutarate- and iron-dependent dioxygenases. Genome Biol. *2*, RESEARCH0007.

Berra, E., Benizri, E., Ginouves, A., Volmat, V., Roux, D., and Pouyssegur, J. (2003). HIF prolyl-hydroxylase 2 is the key oxygen sensor setting low steady-state levels of HIF-1α in normoxia. EMBO J. *22*, 4082–4090.

Bruick, R., and McKnight, S. (2001). A conserved family of prolyl-4-hydroxylases that modify HIF. Science *294*, 1337–1340.

Bryant, J., Farmer, J., Kessler, L.J., Townsend, R.R., and Nathanson, K.L. (2003). Pheochromocytoma: the expanding genetic differential diagnosis. J. Natl. Cancer Inst. *95*, 1196–1204.

Cervellera, M., Raschella, G., Santilli, G., Tanno, B., Ventura, A., Mancini, C., Sevignani, C., Calabretta, B., and Sala, A. (2000). Direct transactivation of the anti-apoptotic gene apolipoprotein J (clusterin) by B-MYB. J. Biol. Chem. *275*, 21055–21060.

Cioffi, C.L., Liu, X.Q., Kosinski, P.A., Garay, M., and Bowen, B.R. (2003). Differential regulation of HIF-1α prolyl-4-hydroxylase genes by hypoxia in human cardiovascular cells. Biochem. Biophys. Res. Commun. *303*, 947–953.

Clifford, S., Cockman, M., Smallwood, A., Mole, D., Woodward, E., Maxwell, P., Ratcliffe, P., and Maher, E. (2001). Contrasting effects on HIF-1α regulation by disease-causing pVHL mutations correlate with patterns of tumourigenesis in von Hippel-Lindau disease. Hum. Mol. Genet. *10*, 1029–1038.

Czyzyk-Krzeska, M.F., and Meller, J. (2004). von Hippel-Lindau tumor suppressor: not only HIF's executioner. Trends Mol. Med. *10*, 146–149.

Darby, C., Cosma, C.L., Thomas, J.H., and Manoil, C. (1999). Lethal paralysis of Caenorhabditis elegans by Pseudomonas aeruginosa. Proc. Natl. Acad. Sci. USA *96*, 15202–15207.

Dechant, G. (2002). Chat in the trophic web: NGF activates Ret by inter-RTK signaling. Neuron *33*, 156–158.

Deckwerth, T.L., and Johnson, E.M., Jr. (1993). Temporal analysis of events associated with programmed cell death (apoptosis) of sympathetic neurons deprived of nerve growth factor. J. Cell Biol. *123*, 1207–1222.

del Peso, L., Castellanos, M.C., Temes, E., Martin-Puig, S., Cuevas, Y., Olmos, G., and Landazuri, M.O. (2003). The von Hippel Lindau/hypoxia-inducible factor (HIF) pathway regulates the transcription of the HIF-proline hydroxylase genes in response to low oxygen. J. Biol. Chem. *278*, 48690–48695.

De Vita, G., Melillo, R.M., Carlomagno, F., Visconti, R., Castellone, M.D., Bellacosa, A., Billaud, M., Fusco, A., Tsichlis, P.N., and Santoro, M. (2000). Tyrosine 1062 of RET-MEN2A mediates activation of Akt (protein kinase B) and mitogen-activated protein kinase pathways leading to PC12 cell survival. Cancer Res. *60*, 3727–3731.

Edwards, S.N., and Tolkovsky, A.M. (1994). Characterization of apoptosis in cultured rat sympathetic neurons after nerve growth factor withdrawal. J. Cell Biol. *124*, 537–546.

Epstein, A., Gleadle, J., McNeill, L., Hewitson, K., O'Rourke, J., Mole, D., Mukherji, M., Metzen, E., Wilson, M., Dhanda, A., et al. (2001). C. elegans EGL-9 and mammalian homologs define a family of dioxygenases that regulate HIF by prolyl hydroxylation. Cell *107*, 43–54.

Estus, S., Zaks, W.J., Freeman, R.S., Gruda, M., Bravo, R., and Johnson, E.M., Jr. (1994). Altered gene expression in neurons during programmed cell death: identification of c-jun as necessary for neuronal apoptosis. J. Cell Biol. *127*, 1717–1727.

Francois, F., Godinho, M.J., Dragunow, M., and Grimes, M.L. (2001). A population of PC12 cells that is initiating apoptosis can be rescued by nerve growth factor. Mol. Cell. Neurosci. *18*, 347–362.

Gerald, D., Berra, E., Frapart, Y.M., Chan, D.A., Giaccia, A.J., Mansuy, D., Pouyssegur, J., Yaniv, M., and Mechta-Grigoriou, F. (2004). JunD reduces tumor angiogenesis by protecting cells from oxidative stress. Cell *118*, 781–794.

Gimenez-Roqueplo, A.P., Favier, J., Rustin, P., Mourad, J.J., Plouin, P.F., Corvol, P., Rotig, A., and Jeunemaitre, X. (2001). The R22X mutation of the SDHD gene in hereditary paraganglioma abolishes the enzymatic activity of complex II in the mitochondrial respiratory chain and activates the hypoxia pathway. Am. J. Hum. Genet. *69*, 1186–1197.

Greene, L. (1978). Nerve growth factor prevents the death and stimulates the neuronal differentiation of clonal PC12 pheochromocytoma cells in serum-free medium. J. Cell Biol. *78*, 747–755.

Greene, L.A., and Tischler, A.S. (1976). Establishment of a noradrenergic clonal line of rat adrenal pheochromocytoma cells which respond to nerve growth factor. Proc. Natl. Acad. Sci. USA *73*, 2424–2428.

Gunzler, V., and Weidmann, K. (1998). Prolyl 4-hydroxylase inhibitors. In Prolyl Hydroxylase, Protein Disulfide Isomerase, and Other Structurally Related Proteins, N.B. Guzman, ed. (New York: Marcel Dekker, Inc.), pp. 65–95.

Ham, J., Babij, C., Whitfield, J., Pfarr, C.M., Lallemand, D., Yaniv, M., and Rubin, L.L. (1995). A c-Jun dominant negative mutant protects sympathetic neurons against programmed cell death. Neuron *14*, 927–939.

Herault, Y., Chatelain, G., Brun, G., and Michel, D. (1992). V-src-induced-transcription of the avian clusterin gene. Nucleic Acids Res. *20*, 6377–6383.

Hirsila, M., Koivunen, P., Gunzler, V., Kivirikko, K.I., and Myllyharju, J. (2003). Characterization of the human prolyl 4-hydroxylases that modify the hypoxia-inducible factor. J. Biol. Chem. *278*, 30772–30780.

Hoffman, M., Ohh, M., Yang, H., Klco, J., Ivan, M., and Kaelin, W.J. (2001). von Hippel-Lindau protein mutants linked to type 2C VHL disease preserve the ability to downregulate HIF. Hum. Mol. Genet. *10*, 1019–1027.

Holme, E. (1975). A kinetic study of thymine 7-hydroxylase from neurospora crassa. Biochemistry *14*, 4999–5003.

Isaacs, J.S., Jung, Y.J., Mole, D.R., Lee, S., Torres-Cabala, C., Chung, Y.-L., Merino, M., Trepel, J., Zbar, B., Toro, J., et al. (2005). HIF overexpression correlates with biallelic loss of fumarate hydratase in renal cancer: Novel role of fumarate in regulation of HIF stability. Cancer Cell *8*, this issue, 143–153.

Ishii, T., Yasuda, K., Akatsuka, A., Hino, O., Hartman, P.S., and Ishii, N. (2005). A mutation in the SDHC gene of complex II increases oxidative stress, resulting in apoptosis and tumorigenesis. Cancer Res. *65*, 203–209.

Ivan, M., Haberberger, T., Gervasi, D.C., Michelson, K.S., Gunzler, V., Kondo, K., Yang, H., Sorokina, I., Conaway, R.C., Conaway, J.W., and Kaelin, W.G., Jr. (2002). Biochemical purification and pharmacological inhibition of a mammalian prolyl hydroxylase acting on hypoxia-inducible factor. Proc. Natl. Acad. Sci. USA *99*, 13459–13464.

Jin, G., and Howe, P.H. (1997). Regulation of clusterin gene expression by transforming growth factor β. J. Biol. Chem. *272*, 26620–26626.

Kaelin, W.G. (2002). Molecular basis of the VHL hereditary cancer syndrome. Nat. Rev. Cancer *2*, 673–682.

Katsetos, C.D., Del Valle, L., Legido, A., de Chadarevian, J.P., Perentes, E., and Mork, S.J. (2003). On the neuronal/neuroblastic nature of medulloblastomas: a tribute to Pio del Rio Hortega and Moises Polak. Acta Neuropathol. (Berl.) *105*, 1–13.

Kieser, A., Seitz, T., Adler, H.S., Coffer, P., Kremmer, E., Crespo, P., Gutkind, J.S., Henderson, D.W., Mushinski, J.F., Kolch, W., and Mischak, H. (1996). Protein kinase C-zeta reverts v-raf transformation of NIH-3T3 cells. Genes Dev. *10*, 1455–1466.

Kim, W.Y., and Kaelin, W.G. (2004). Role of VHL gene mutation in human cancer. J. Clin. Oncol., in press.

Kondo, K., Klco, J., Nakamura, E., Lechpammer, M., and Kaelin, W.G. (2002). Inhibition of HIF is necessary for tumor suppression by the von Hippel-Lindau protein. Cancer Cell *1*, 237–246.

Kondo, K., Kim, W.Y., Lechpammer, M., and Kaelin, W.G., Jr. (2003). Inhibition of HIF2α is sufficient to suppress pVHL-defective tumor growth. PLoS Biol. *1*, e83. 10.1371/journal.pbio.0000083

Lenaz, G., Baracca, A., Carelli, V., D'Aurelio, M., Sgarbi, G., and Solaini, G. (2004). Bioenergetics of mitochondrial diseases associated with mtDNA mutations. Biochim. Biophys. Acta *1658*, 89–94.

Lipscomb, E., Sarmiere, P., Crowder, R., and Freeman, R. (1999). Expression of the SM-20 gene promotes death in nerve growth factor-dependent sympathetic neurons. J. Neurochem. *73*, 429–432.

Lipscomb, E., Sarmiere, P., and Freeman, R. (2001). SM-20 is a novel mitochondrial protein that causes caspase-dependent cell death in nerve growth factor-dependent neurons. J. Biol. Chem. *276*, 11775–11782.

Lonergan, K.M., Iliopoulos, O., Ohh, M., Kamura, T., Conaway, R.C., Conaway, J.W., and Kaelin, W.G. (1998). Regulation of hypoxia-inducible mRNAs by the von Hippel-Lindau protein requires binding to complexes containing elongins B/C and Cul2. Mol. Cell. Biol. *18*, 732–741.

Maher, E.R., and Eng, C. (2002). The pressure rises: update on the genetics of phaeochromocytoma. Hum. Mol. Genet. *11*, 2347–2354.

Maher, E., and Kaelin, W.G. (1997). von Hippel-Lindau disease. Medicine *76*, 381–391.

Marxsen, J.H., Stengel, P., Doege, K., Heikkinen, P., Jokilehto, T., Wagner, T., Jelkmann, W., Jaakkola, P., and Metzen, E. (2004). Hypoxia-inducible factor-1 (HIF-1) promotes its degradation by induction of HIF-α-prolyl-4-hydroxylases. Biochem. J. *381*, 761–767.

Maxwell, P., Weisner, M., Chang, G.-W., Clifford, S., Vaux, E., Pugh, C., Maher, E., and Ratcliffe, P. (1999). The von Hippel-Lindau gene product is necessary for oxygen-dependent proteolysis of hypoxia-inducible factor α subunits. Nature *399*, 271–275.

McLennan, H.R., and Degli Esposti, M. (2000). The contribution of mitochondrial respiratory complexes to the production of reactive oxygen species. J. Bioenerg. Biomembr. *32*, 153–162.

Menzies, K., Liu, B., Kim, W.J., Moschella, M.C., and Taubman, M.B. (2004). Regulation of the SM-20 prolyl hydroxylase gene in smooth muscle cells. Biochem. Biophys. Res. Commun. *317*, 801–810.

Messam, C.A., and Pittman, R.N. (1998). Asynchrony and commitment to die during apoptosis. Exp. Cell Res. *238*, 389–398.

Metzen, E., Berchner-Pfannschmidt, U., Stengel, P., Marxsen, J.H., Stolze, I., Klinger, M., Huang, W.Q., Wotzlaw, C., Hellwig-Burgel, T., Jelkmann, W., et al. (2003). Intracellular localisation of human HIF-1α hydroxylases: implications for oxygen sensing. J. Cell Sci. *116*, 1319–1326.

Murata, H., Tajima, N., Nagashima, Y., Yao, M., Baba, M., Goto, M., Kawamoto, S., Yamamoto, I., Okuda, K., and Kanno, H. (2002). Von Hippel-Lindau tumor suppressor protein transforms human neuroblastoma cells into functional neuron-like cells. Cancer Res. *62*, 7004–7011.

Myllyla, R., Tuderman, L., and Kivirikko, K.I. (1977). Mechanism of the prolyl hydroxylase reaction. 2. Kinetic analysis of the reaction sequence. Eur. J. Biochem. *80*, 349–357.

Nakagawara, A. (2001). Trk receptor tyrosine kinases: a bridge between cancer and neural development. Cancer Lett. *169*, 107–114.

Neumann, H., Bausch, B., McWhinney, S., Bender, B., Gimm, O., Franke, G., Schipper, J., Klisch, J., Altehoefer, C., Zerres, K., et al. (2002). Germline mutations in nonsyndromic pheochromocytoma. N. Engl. J. Med. *343*, 1459–1466.

Ohh, M., Park, C.W., Ivan, M., Hoffman, M.A., Kim, T.-Y., Huang, L.E., Chau, V., and Kaelin, W.G. (2000). Ubiquitination of hypoxia-inducible factor requires direct binding to the β-domain of the von Hippel-Lindau protein. Nat. Cell Biol. *2*, 423–427.

Okuda, H., Hirai, S., Takaki, Y., Kamada, M., Baba, M., Sakai, N., Kishida, T., Kaneko, S., Yao, M., Ohno, S., and Shuin, T. (1999). Direct interaction of the β-domain of VHL tumor suppressor protein with the regulatory domain of atypical PKC isotypes. Biochem. Biophys. Res. Commun. *263*, 491–497.

Okuda, H., Saitoh, K., Hirai, S., Iwai, K., Takaki, Y., Baba, M., Minato, N., Ohno, S., and Shuin, T. (2001). The von Hippel-Lindau tumor suppressor protein mediates ubiquitination of activated atypical protein kinase C. J. Biol. Chem. *276*, 43611–43617.

Pal, S., Claffey, K., Dvorak, H., and Mukhopadhyay, D. (1997). The von Hippel-Lindau gene product inhibits vascular permeability factor/vascular endothelial growth factor expression in renal cell carcinoma by blocking protein kinase C pathways. J. Biol. Chem. *272*, 27509–27512.

Palmada, M., Kanwal, S., Rutkoski, N.J., Gustafson-Brown, C., Johnson, R.S., Wisdom, R., and Carter, B.D. (2002). c-jun is essential for sympathetic neuronal death induced by NGF withdrawal but not by p75 activation. J. Cell Biol. *158*, 453–461.

Peterson, S., and Bogenmann, E. (2004). The RET and TRKA pathways collaborate to regulate neuroblastoma differentiation. Oncogene *23*, 213–225.

Schlingensiepen, K.H., Wollnik, F., Kunst, M., Schlingensiepen, R., Herdegen, T., and Brysch, W. (1994). The role of Jun transcription factor expression and phosphorylation in neuronal differentiation, neuronal cell death, and plastic adaptations in vivo. Cell. Mol. Neurobiol. *14*, 487–505.

Schofield, C.J., and Ratcliffe, P.J. (2004). Oxygen sensing by HIF hydroxylases. Nat. Rev. Mol. Cell Biol. *5*, 343–354.

Schofield, C.J., and Zhang, Z. (1999). Structural and mechanistic studies on 2-oxoglutarate-dependent oxygenases and related enzymes. Curr. Opin. Struct. Biol. *9*, 722–731.

Selak, M.A., Armour, S.M., Mackenzie, E.D., Boulahbel, H., Watson, D.G., Mansfield, K.D., Pan, Y., Simon, M.C., Thompson, C.B., and Gottlieb, E. (2005). Succinate links TCA cycle dysfunction to oncogenesis by inhibiting HIF-α prolyl hydroxylase. Cancer Cell *7*, 77–85.

Standaert, M.L., Sajan, M.P., Miura, A., Kanoh, Y., Chen, H.C., Farese, R.V., Jr., and Farese, R.V. (2004). Insulin-induced activation of atypical protein kinase C, but not protein kinase B, is maintained in diabetic (ob/ob and Goto-Kakazaki) liver. Contrasting insulin signaling patterns in liver versus muscle define phenotypes of type 2 diabetic and high fat-induced insulin-resistant states. J. Biol. Chem. *279*, 24929–24934.

Straub, J.A., Lipscomb, E.A., Yoshida, E.S., and Freeman, R.S. (2003). Induction of SM-20 in PC12 cells leads to increased cytochrome c levels, accumulation of cytochrome c in the cytosol, and caspase-dependent cell death. J. Neurochem. *85*, 318–328.

Taylor, M.S. (2001). Characterization and comparative analysis of the EGLN gene family. Gene *275*, 125–132.

Tsui-Pierchala, B.A., Milbrandt, J., and Johnson, E.M., Jr. (2002). NGF utilizes c-Ret via a novel GFL-independent, inter-RTK signaling mechanism to maintain the trophic status of mature sympathetic neurons. Neuron *33*, 261–273.

Vandenplas, M.L., Mamidipudi, V., Lamar Seibenhener, M., and Wooten, M.W. (2002). Nerve growth factor activates kinases that phosphorylate atypical protein kinase C. Cell. Signal. *14*, 359–363.

Vogel, K.S., Brannan, C.I., Jenkins, N.A., Copeland, N.G., and Parada, L.F. (1995). Loss of neurofibromin results in neurotrophin-independent survival of embryonic sensory and sympathetic neurons. Cell *82*, 733–742.

Wei, W., Jin, J., Schlisio, S., Harper, J.W., and Kaelin, W.G., Jr. (2005). The v-Jun point mutation allows c-Jun to escape GSK3-dependent recognition and destruction by the Fbw7 ubiquitin ligase. Cancer Cell *8*, 25–33.

Wooten, M.W., Vandenplas, M.L., Seibenhener, M.L., Geetha, T., and Diaz-Meco, M.T. (2001). Nerve growth factor stimulates multisite tyrosine phosphorylation and activation of the atypical protein kinase C's via a src kinase pathway. Mol. Cell. Biol. *21*, 8414–8427.

Xia, Z., Dickens, M., Raingeaud, J., Davis, R.J., and Greenberg, M.E. (1995). Opposing effects of ERK and JNK-p38 MAP kinases on apoptosis. Science *270*, 1326–1331.

Yankovskaya, V., Horsefield, R., Tornroth, S., Luna-Chavez, C., Miyoshi, H., Leger, C., Byrne, B., Cecchini, G., and Iwata, S. (2003). Architecture of succinate dehydrogenase and reactive oxygen species generation. Science *299*, 700–704.

Yu, Y., Platoshyn, O., Zhang, J., Krick, S., Zhao, Y., Rubin, L.J., Rothman, A., and Yuan, J.X. (2001). c-Jun decreases voltage-gated K^+ channel activity in pulmonary artery smooth muscle cells. Circulation *104*, 1557–1563.

Zbar, B., Kishida, T., Chen, F., Schmidt, L., Maher, E.R., Richards, F.M., Crossey, P.A., Webster, A.R., Affara, N.A., Ferguson-Smith, M.A., et al. (1996). Germline mutations in the von Hippel-Lindau (VHL) gene in families from North America, Europe, and Japan. Hum. Mutat. *8*, 348–357.

Zimmer, M., Doucette, D., Siddiqui, N., and Iliopoulos, O. (2004). Inhibition of hypoxia-inducible factor is sufficient for growth suppression of VHL–/– tumors. Mol. Cancer Res. *2*, 89–95.